Effects of Zr/Ti ratio and sintering temperature on Structural and electrical properties of PFN-PNN-PZTceramics near the morphotropic phase boundary

Loubna Ben Amor[1]✉, Ahmed Boutarfaia[1, 2], Omar Bentouila[1, 3]

1 Département de Sciences de la Matière, Université KasdiMerbah-Ouargla, BP.511, RP-Ouargla, (30000), Algérie

2 Laboratoire de Chimie Appliquée, Université de Biskra, BP.145, RP-Biskra (07000), Algérie

3 Équipe Optoélectronique, Laboratoire LENREZA, Université Kasdi Merbah-Ouargla,30000 Ouargla, Algérie

Received 6 June 2017
Published online: 24 May 2018

Keywords
PFN-PNN-PZT
Sintering temperature
Morphotropic phase boundary
Piezoelectric
Properties
Dielectric properties

Abstract: 0.05Pb[$Fe_{1/2}$ $Nb_{1/2}$]O_3-0.05Pb[$Ni_{1/3}Nb_{2/3}$]O_3-0.90Pb[$Zr_xTi_{(1-x)}$]O_3 [PFN-PNN-PZT] quaternary piezoelectric ceramics with varying Zr/Ti ratios located near the morphotropic phase boundary (MPB) were prepared by a conventional mixed-oxide route. The samples structure was determined by X-ray diffractometry which indicate that the phase structure, of sintered PFN-PNN-PZT ceramics, was transformed from tetragonal to rhombohedral with Zr/Ti ratio increased in system. The effect of Zr/Ti ratio and sintering temperature on the structure and piezoelectric properties of our simples were investigated. The new MPB in this quaternary system with optimum piezoelectric properties was found at x = 0.51-0.53. The dependence of the piezoelectric coefficient (d_{31}), electromechanical coupling factor (kp) and the dielectric constant (ε) on the Zr/Ti ratio shows a pronounced maximum of d_{31} = 141* 10^{-12} C/N, kp= 0.64 and ε = 850 at Zr/Ti : 51/49. As the Zr/Ti ratio increases, the *Tc*of PFN-PNN-PZT ceramics decreases and consequently the peak in the dielectric spectrum corresponding to the *Tc* moves towards room temperature. A *Tc* of 360 °C is obtained when Zr/Ti: 51/49..

1. Introduction

Lead zirconatetitanatePb(Zr_x,Ti_{1-x})O_3 (PZT), ceramics based on a continuous solid solution system of perovskite ferroelectric $PbTiO_3$ and antiferroelectric $PbZrO_3$, are known as an important piezoelectric materials (Jaffeet al. 1971 and Sriram et al. 2010). These materials have been studied extensively since the discovery of the miscibility of lead titanate and lead zirconate early in the 1950's (Jaffeet al. 1971).

PZT ceramics have been used in several technological applications such as ultrasonic sensors, high energy capacitors, piezoelectric actuators, non-volatile random access memories (NVRAMs), and photoelectric devices (Haertling 1999, Nonaka et al.2000, Ledermann et al. 2004, Chauhan et al. 2015 and Malik et al. 2016). In order to enhance its piezoelectric properties, both of the effects of different processing conditions (Kakegawa et al. 1977, Hiremath et al. 1983, Saha and Agrawal 1992, Praveen et al. 2015 and Wongmaneerung et al. 2016) and substitutions of various dopants (Gerson and Jaffe 1963, Jaffe et al. 1971,Takahashi 1982, Fu et al. 1986, Tadon and Singh 1994, Lee and Lee 2006 and Amarande et al. 2016) of different ionic sizes and valences have been studied. Doping with different element changes the physical and chemical properties of PZT ceramics. Due the broad range of possible isomorphism in the perovskite structure of ABO_3, PZT ceramics can be accept dopants with different valences into both A-site (Pb-site) and B-site (Zr/Ti –site) of the lattice (Gonnard et al.1978 and Nguyen et al. 2014). Based on aliovalent substituents in the compound, dopants can be classified into two types: donors (higher valence ions) and acceptors (lower valence ions. PZT ceramics can be form a “soft” PZTs, when doped with donor such as La^{3+} (Kulcsar 1959, Haertling and Land 1971, Dai et al. 1996 and Singh et al. 2006) for A-site, and Nb^{5+}, (Kulcsar 1959, Atkin et al. 1971 and Castro et al. 2000) for B-site which lead to creation of site A vacancies, or a “hard” PZTs, when doped with acceptor like Na^+ at A-site and Ni^{2+}, Fe^{3+} at B-site to create some oxygen vacancies in the lattice (Weston et al. 1969, Karapuzha et al. 2016 and Yu et al. 2017). Soft PZTs have high piezoelectric characteristicsand are easy to pole. Conversely, hard PZTs are difficult to pole and have low piezoelectric characteristics (Shrout and Zhang 2007). Doping PZT with Nb^{5+} increases the electric permittivity and piezoelectric coefficients (Bornand et al. 2001), but PZT doped with iron presents lower dielectric constant and loss constant (Raí et al. 2005).

Furthermore, the morphotropic phase boundary (MPB) (Wilkinson et al. 1998) is an essential parameter to be considered because in this region, tetragonal and rhombohedral phases coexist, and consequently the properties of PZT are improved (dielectric and piezoelectric properties).

The aim of the present work is to study the dielectric and piezoelectric properties for PFN-PNN-PZT quaternary ceramics.

✉Corresponding author. E-mail address: loubnabenamor@yahoo.fr

Aneffort has been made to determine the MPB phasecontents with variations in the Zr/Ti ratio**.** The effects of Zr/Ti ratio on the properties of sintered PFN-PNN-PZT quaternary system ceramics were investigated systematically.

2. Experimental

Samples with general formula : $0.05Pb[Fe_{1/2}\ Nb_{1/2}]O_3$-$0.05Pb[Ni_{1/3}Nb_{2/3}]O_3$-$0.90Pb[Zr_xTi_{(1-x)}]O_3$($0.49 \leq x \leq 0.55$) were synthesized from starting materials Pb_3O_4 (99.90%), ZrO_2 (99.90%), TiO_2 (99.90%), Fe_2O_3 (98%), NiO (99.90%) and Nb_2O_5 (99.6%). Each mixture of the starting powders was mixed in a centrifugal mill with absolute alcohol using an agate ball for 3h. The powders were then calcined at 800 °C for 2h at heating and cooling rates of 2°C.min^{-1}. The powders were molded by the pressure of 150 MPa in 12 mm in diameter and about 1 mm in thickness. The pressed disks were covered with alumina crucible and then sintered at 1180 °C for 2 h. To limit PbO loss from the pellets, a PbO-rich atmosphere was maintained by placing a $PbZrO_3$ inside the crucible.

For phase characterization, the crystal structure were determined from XRD (XRD, Siemens D500 diffractometer) patterns, that were recorded with CuKα radiation (λ= 0.15405 nm). The compositions of the PFN-PNN-PZT phases were identified by analysis of the peaks [(0 0 2)T, (2 0 0)R, (2 0 0)T] in the 2θ range (5°-60°). The tetragonal (T), rhombohedral (R) and tetragonal-rhombohedral (T+R) phases were characterized and their lattice parameters were calculated. The size, shape and distribution of the grains were analyzed using Scanning electron microscope (*Quanta TM 250*). The bulk densities of sintered samples were determined by the Archimedes method in water.

For measuring the piezoelectric characteristics, the specimens were polished to 2 mm thickness and then electrodeposited with Ag paste. The pellets are carried out at 110 °C in a silicone oil bath by applying fields of 2.5kV cm^{-1} for 45 min. All samples were aged for 24 h prior to measuring the piezoelectric and dielectric properties.

The dielectric properties (from a room temperature to 450°C) of the poled ceramics were investigated using an automatic (LCR) meter at 1 kHz. The piezoelectric properties of the specimens were calculated by the resonance-antiresonance method using an impedance analyzer.

3. Results and discussion

3.1 Phase analysis and Morphological characterization of the PFN-PNN-PZT

To identify the phase formation and the crystal structure, the powders with optimum sintering temperature were examined by XRD. Figure 1 displays XRD patterns of $0.05Pb[Fe_{1/2}\ Nb_{1/2}]O_3$-$0.05Pb[Ni_{1/3}Nb_{2/3}]O_3$-$0.90Pb[Zr_xTi_{(1-x)}]O_3$ ceramics with various Zr/Ti ratio at 49/51, 51/49, 53/47and 55/45 sintered at 1180°C.

It is seen that by varying the Zr/Ti ratio, one can alter the phase fraction of the phases present in the system and thereby control the properties which depend on the relative amount of phases. All peaks are well matched with the Perovskite structure. The tetragonal (T), rhombohedral

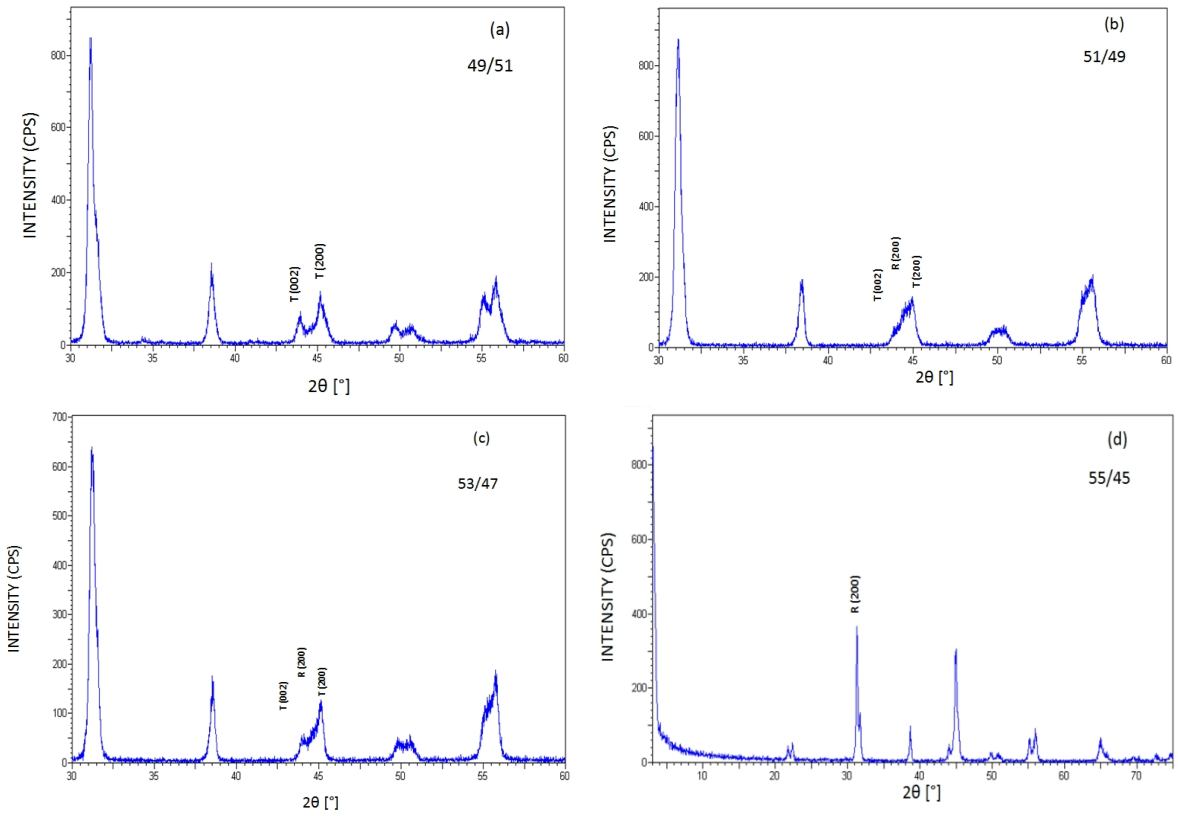

Fig. 1.XRD patterns of sintered PFN-PNN-PZTceramics with a varying Zr addition: (a) 49; (b) 51; (c); 53 and (d); 55 sintered at 1180°C.

(R) and tetragonal-rhombohedral(T–R) phase were identified by an analysis of the peaks of tetragonal (002),tetragonal (200), rhombohedral (200) in the 2θ range of 43° to 47°. A transition from the tetragonal to the rhombohedral phase is observed as Zr/Ti ratio increases. Triplet peak indicates that the samples are consists of a mixture of tetragonal and rhombohedral phases.

For Zr/Ti : 49/51, the doublet nature of the (002) and (200) lines are clearly seen, the system is in a tetragonal phase, when the Zr/Ti was $0.51 \leq x \leq 0.53$, morphotropic phase boundary (MPB), coexisting rhombohedral and tetragonal phases were observed and when Zr/Ti : 55/45 the phase rhombohedral observed.

The evolution of lattice parameters of the quaternary system PZT-PFNN as a function of composition is shown in Figure 2. The tetragonal phase shows that the parameter a_T increases and c_T decreases with the increase in the concentration of Zr. As the concentration of Zr increases, the parameter of the rhombohedral phase a_R decreases. The variation of these parameters is related to the distortion of the tetragonal structure, defined by the c_T/a_T ratio, which decreases with increasing Zr content. The influence of the substitution of Zr/Ti on the parameters of the structure can be explained by the difference between the ionic rays of Zr and Ti (0.68 and 0.79 Å respectively) (Chen et al. 2007). This cannot provide a complete homogeneity in the solid solutions containing both tetragonal and rhombohedral phases.

Figure 3 shows the SEM images of PZT-PFNN (49/51, 51/49, 53/47 and 55/45) ceramics sintered at 1180 °C. All the sintered ceramics appear to be very dense and of a homogeneous granular structure. At first sight, the samples appear homogeneous and there does not seem to be any grains of the pyrochlore phase which are identifiable by their pyramidal form (Kighelman 2001; Ghasemifard et al. 2009).

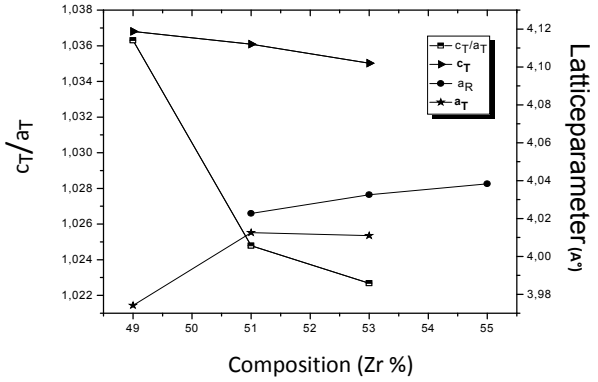

Fig. 2. Variation of the unit cell dimensions and ratio c_T/a_T with different Zr/Ti ratios in the PZT–PFN–PNN samples

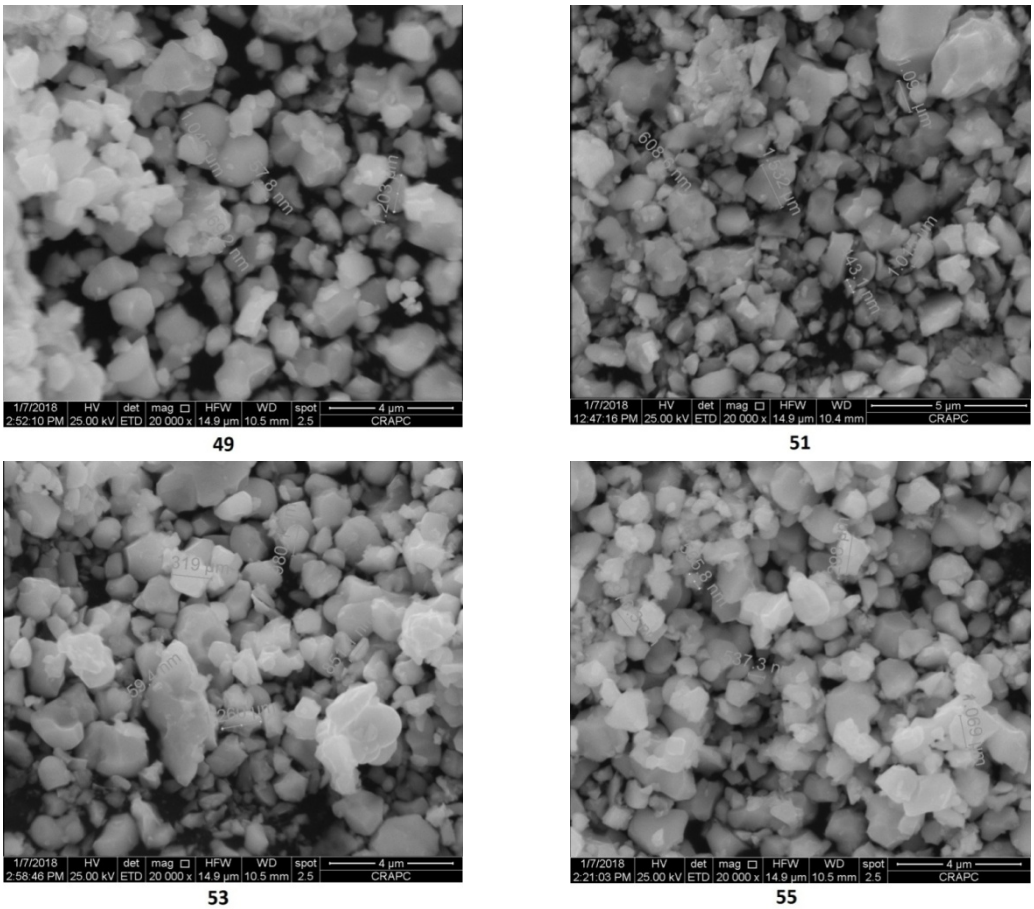

Fig. 3. SEM micrographs of PFN–PNN-PZT specimens sintered at 1180°C with different Zr/Ti ratios.

Table 1. The average grain size of PZT-PFNN ceramics.

Composition	49/51	51/49	53/47	55/45
Average size (µm)	1.203	1.532	1.319	1.298

The ruptures with the grain boundaries are synonymous with a good sintering. It is observed that the average grain size of the four samples varies between 1.203µm and 1.532 µm (Table 1), and the grain distribution and uniform.

Large values of the average grain size for the two samples 51/49 and 53/47 are noted at the same sintering temperature (1180 ° C).This was due to the coexistence of the two phases in the latte. The increase in grain size may have caused the decrease of oxygen deficiency in the PZT (Ohtaka at al. 1995).

Figure 4 and Figure 5 shows the variation of bulkdensity and porosity with the compositions at variation sintering temperature (1100, 1150, and 1180° C). The porosity decreases when the sintering temperature. Meanwhile, the density of specimens increased, and shows the maximum value of 7.4 at 51/49 with 1180° C, so the optimum temperature of sintering is 1180 °C. The quality of the material increases with increasing density and it increases with increasing the sintering temperature (Boutarfaia 2000).

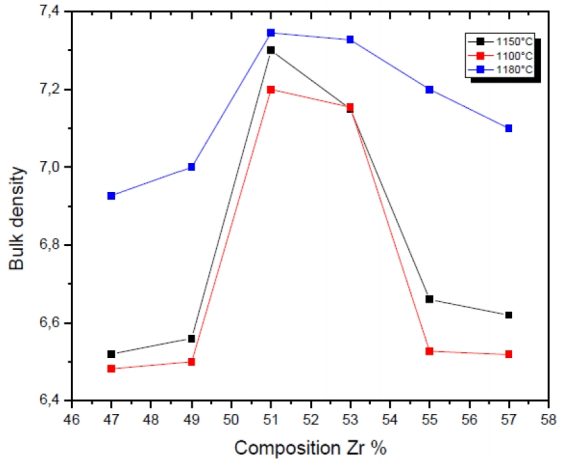

Fig. 4. Change in bulk density as functions of Zr in the composition and sintering temperature

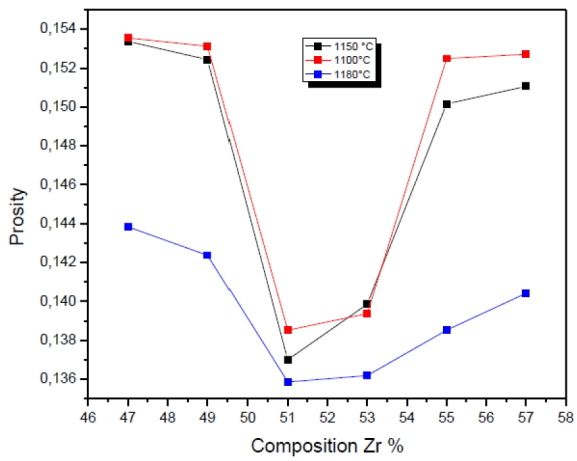

Fig. 5. Change in porosity as functions of Zr in the composition and sintering temperature

3.2 Dielectric characterization of the PFN-PNN-PZT

Figure 6 and Figure 7 shows the temperature and composition dependence of the dielectric constant of PFN-PNN-PZT ceramics with different sintering temperatures (1100, 1150 and 1180 °C) at 1 kHz. For the three temperatures of sintering 1100, 1150 and 1180 °C, we can observed that the permittivity increases gradually with the increase in the composition and takes a maximum for the sample with Zr/Ti = 51/49 included in the morphotropic phase boundary (MPB) at the temperature 1180 °C and then decreases. The region around the dielectric peak is broadened. The broadening or diffuseness of peak occurs mainly due to compositional fluctuation and/or substitution disordering in the arrangement of cations in one or more crystallographic sites of the PFN-PNN-PZT structure. Because theCurietemperatureof$PbZrO_3$ (Tc = 230 °C) islower than $PbTiO_3$ (Tc = 490 °C), increasingtheZr/Tiratio causesthe Tc of the PFN–PNN–PZTceramicstodecrease.Consequentlythe peak inthedielectricspectrumcorrespondingtothe Tc moves towards roomtemperature,asshownin Figure 8. Thedielectric constant peaks are in the range of 6,000–13,000. Thehighest dielectric constantpeakisachievedinthesamplewith x=0.51, which givesa Tc of 360°C.

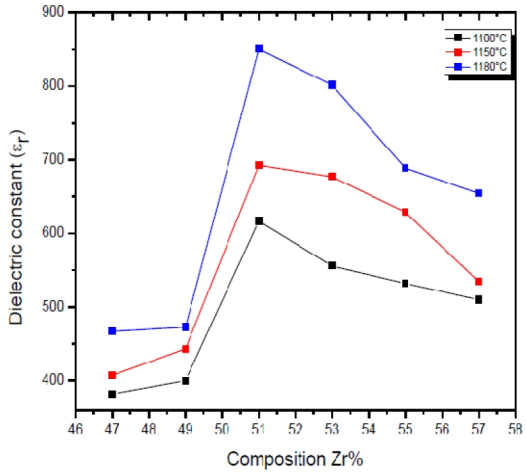

Fig. 6. Dielectric Constant (ε) as a function of the composition (Zr%)

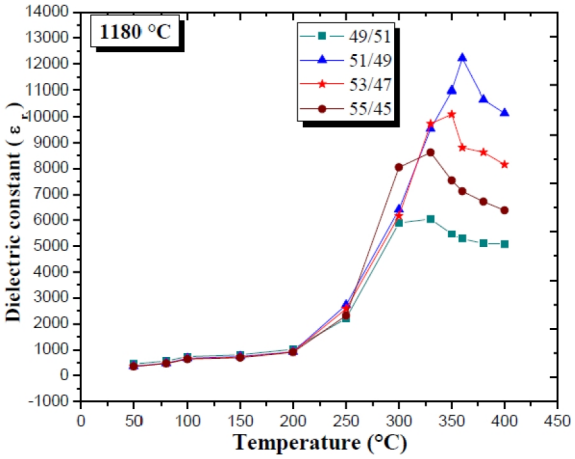

Fig. 7. Dielectric Constant (ε) as a function of the temperature.

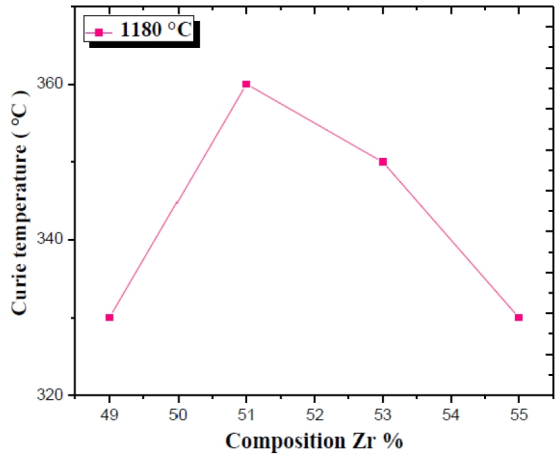

Fig. 8. Variation of Curie temperature as functions of composion (Zr%) sintered at 1180°C.

The variation of dielectric loss (tan δ) with temperature and composition (at room temperature, 1 kHz) sintered at various temperatures (1100, 1150, and 1180 °C) are shown in Figure 9 and Figure 10 respectively. The dielectric loss exhibits a peak near the transition temperature. The dielectric loss tangent is of the same order at room temperature for all the samples, while near the transition temperature region the dielectric loss tangent has a lower value for lower Zr compositions.

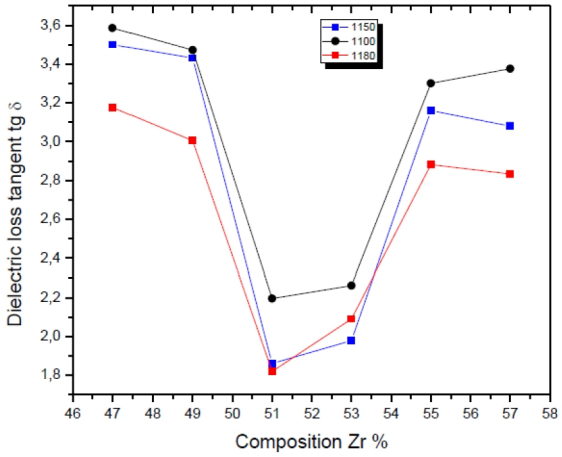

Fig. 9. Dielectric loss tangent (tgδ) as a function of the composition (Zr%).

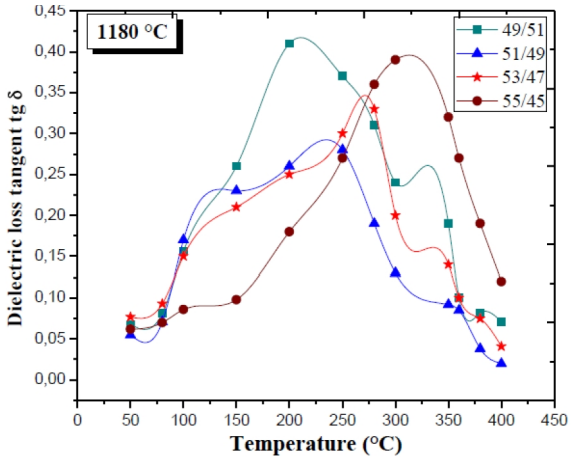

Fig. 10. Dielectric loss tangent (tgδ) as a function of the temperature.

3.3. Piezoelectric properties

Figure 11 and Figure 12 shows respectively the variation of piezoelectric coefficient (d_{31}) and electromechanical coupling factor (*kp*) as a function of the Zr/Ti ratio sintered at 1180 °C. That as the Zr/Ti ratio increases; the value of d_{31} represents a peak of 141* 10^{-12} C/N at Zr/Ti ratio of 51/49; and when Zr/Ti ratio is further increased, the value of d_{31} decreases. Similar to the values of d_{31}, the *kp* values of the ceramic specimens form a parabola shape, and reach the peak value (0.64) at the same Zr/Ti ratio of 51/49. This maximum of piezoelectric activity can be explained as folow: during the polarization of material, the degree of domain alignment increases and becomes higher in the area of co-existence of the tetragonal and rhombohedral phases. This idea was underlined and confirmed by Heywang (1965) and Isupov (1975).

Additionally, a small amount of doping Nb^{5+} will increase the densification and reduce the grain sizes of ceramics during the sintering procedure (Chu et al. 2004, Pereira et al.2001 and Sakaki et al. 2001). These phenomena can all be observed in our results.

The dielectric and piezoelectric properties of the samples also confirm that the MPB in PFN-PNN-PZT quaternary piezoelectric ceramics is close to $x = 0.51$. It can be concluded from this that

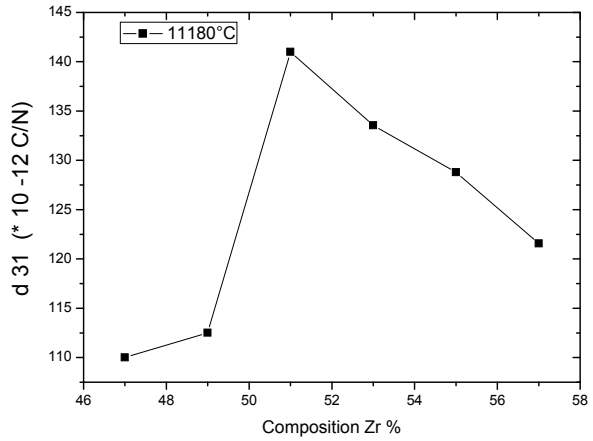

Fig. 11. Variation of piezoelectric constant (d_{31}) as functions of composion (Zr%) sintered at 1180°C.

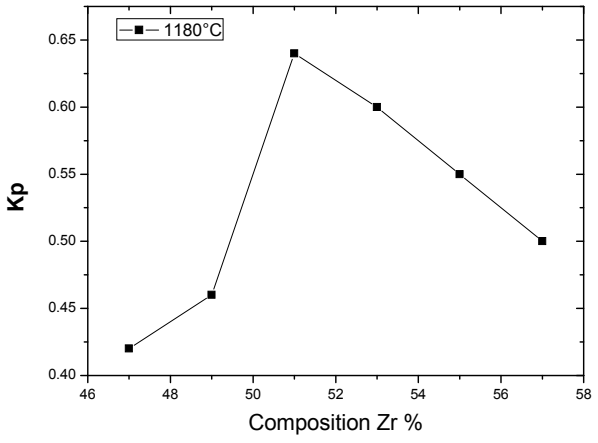

Fig. 12. Variation of electromechanical coupling factor (k_p) as functions of composion (Zr%) sintered at 1180 °C.

the Zr/Ti ratio plays an important role in determining the material properties of the system and can be tuned to retain the MPB in a system. This is presumably attributed to the effect of hard and soft doping in the chosen PFN-PNN-PZT system. Our complex doped by Ni^{+2} , Fe^{3+} (hard) and Nb^{+5} (soft) at the B-site produces materials with the advantages of both soft and hard ceramics.

4. Conclusion

In this study, $0.05Pb[Fe_{1/2}Nb_{1/2}]O_3$-$0.05Pb[Ni_{1/3}Nb_{2/3}]O_3$-$0.90Pb[Zr_xTi_{(1-x)}]O_3$ ceramics ($0.49 \leq x \leq 0.55$) were successfully prepared using a solid-state mixed oxide technique at different sintering temperature. The phase structure of system was transformed from tetragonal to rhombohedral with an increase of Zr/Ti ratio. X-ray diffraction studies revealed that PFN-PNN-PZT showed a MPB region ($0.51 \leq x \leq 0.53$). The ratio of Zr/Ti and the sintering temperature strongly affects the electrical properties of PFN-PNN-PZT ceramics. A transition from tetragonal to rhombohedral phase and density were observed as Zr/Ti ratio increased, and greatly important improvement in electrical properties when sintering temperature and ratio of Zr/Ti increase. Scanning electron micrographs of sintered ceramic surfaces (at 1180°C) showed the dense and uniform microstructure for composition close to MPB (Zr/Ti = 51/49) with apparent density of 7.4 g/cm3 . The optimum dielectric constant (ε =13108) and piezoelectric properties (tan δ = 0.012,d_{31} = 141* 10^{-12} C/N and kp = 0.64) were observed for the composition sintered at 1180 °C that contains Zr/Ti ratio of 51/49, which could be suitable for high-power applications.

References

Amarande, L., C. Miclea, M. Cioangher, M.N. Grecu& I. Pasuk (2016) Effects of vanadium doping on sintering conditions and functional properties of Nb-Li co-doped PZT ceramics. Comments on Li location.Journal of Alloys and Compounds 685: 159-166.

Atkin, R. B., R. L. Holman, R. M. Fulrath (1971) Substitution of Bi and Nb Ions in Lead Zirconate-Titanate.Journal of the American Ceramic Society 54: 113-115.

Bornand, V., D. Granier, P. Papet& E. Philippot (2001) Elaboration and characterization ofNb-doped PZT ceramics.Annalesde Chimie Science des Materiaux.26(1): 135-139.

Boutarfaia, A. (2000) Investigation of Co-Existence Region in Lead Zirconate-Titanate Solid Solutions: X-Ray Diffraction Studies. Ceramic International 26(6): 583-587.

Castro, J., T. de los Rios, L. Fuentes (2000) Synthesis and Characterization of Nb-Doped PZT FerroPiezoelectric Ceramics. Materials and Manufacturing Processes 15(2): 301-310.

Chauhan, A., S. Patel, R. Vaish, C.R. Bowen (2015) Anti-Ferroelectric Ceramics for High Energy Density Capacitors. Materials 8(12):8009–8031.

Chen, C. Y., Y. Hu, H. L. Lin, W. Y.Wei (2007) Influence of the sintering temperature on phase development in PMnN–PZT ceramics. Ceramics International 33(2):263–268.

Chu, S. Y., T. Y. Chen, I.T. Tsai (2004) Effects of poling field on the piezoelectric and dielectric properties of Nb additive PZT-based ceramics and their applications on SAW devices. Materials Letters 58 (5):752–756.

Dai, X., Z. Xu, D. Viehland (1996) Long-time relaxation from relaxor to normal ferroelectric states in Pb0.91La0.06 (Zr0.65Ti0.35 O3.Journal of the American Ceramic Society 79(7):1957-1960.

Fu, S. L., S. Y.Cheng, C.C.Wei (1986) Effects of doping pairs on the preparation and dielectricity of PLZT ceramics. Ferroelectrics 67 (1): 93-102.

Gerson, R., H. Jaffe (1963) Electric Conductivity in Lead TitanateZirconate Ceramics. Journal of Physics and Chemistry of Solids 24(8): 979–284.

Ghasemifard, M., S. M. Hosseini, M. M. Bagheri-Mohagheghi, N.Shahtahmasbi (2009) Structure comparison of PMN-PT and PMN-PZT nanocrystal prepared by gel-combustion method at optimized temperatures. Physica E: Low-dimensional Systems and Nanostructures 41(9)1701-1706

Gonnard, P., M. Troccaz (1978) Dopant distribution between A and B sites in the PZT ceramics of type ABO_3.Journal of Solid State Chemistry 23(3-4): 321–326.

Haertling, G. H. (1999) Ferroelectric Ceramics: History and Technology. Journal of the American Ceramic Society 82 (4): 797–818.

Haertling, G. H., C.E. Land (1971) Hot-Pressed (Pb,La)(Zr,Ti)O_3 Ferroelectric Ceramics for Electrooptic Applications. Journal of the American Ceramic Society 54 (1):1-11.

Heywang, W. (1965) Ferroelektrizität in PerowskitischenSystemen und IhreTechnischenAnwendungen.Zeitschriff Fur AngewandtePhysik19: 473-481.

Hiremath, B. V., A. Kingon, J.V. Biggers (1983) Reaction sequence in the formation of lead zirconate-lead titanate solid solution: Role of raw materials. Journal of the American Ceramic Society 66(11): 790–793.

Isupov, V. A. (1975) Comments on the paper “X-ray study of the PZT solid solutions near the morphotropic phase transition”. Solid State Communication 17(11): 1331-1333.

Izyumskaya, N., Y. I.Alivov, S. J.Cho, H. Morkoç, H. Lee & Y. S. Kang (2007) Processing, Structure, Properties, and Applications of PZT Thin Films. Critical Reviews in Solid State and Materials Science 32(3-4): 111-202.

Jaffe, B., R. Cook Jr., H. Jaffe (1971) Chapter 7: Solide Solutions of Pb(Ti, Zr, Sn, Hf)O_3, in Piezoelectric Ceramics, Ed. B. Jaffe, W. R. Cook, and H. Jaffe , New York, Academic Press, pp.135-183.

Kakegawa, K., J. Mohri (1977) A compositional fluctuation and properties of Pb(Zr, Ti)O_3.Solid State Communications 24(11):769-772.

Karapuzha, A. S., N. K. James, H. Khanbareh, S. van der Zwaag& W.A. Groen (2016) Structure, dielectric and piezoelectric properties of donor doped PZT ceramics across the phase diagram. Ferroelectrics504(1): 160-171.

Kighelman, Z. (2001) films minces relaxeur-ferroélectriques à base de Pb (Mg1/3 Nb2/3) : élaboration, propriétés diélectriques et électromécaniques. PhD. Thesis, Ecole Polytechniques de Lausanne. France.

Kulcsar, F. (1959) Electromechanical Properties of Lead TitanateZirconate Ceramics Modified with Certain Three-or Five-Valent Additions. Journal of The American Ceramic Society 42: 343-349.

Ledermann, N., P. Muralt, J. Baborowski, M.Forster and J-P.Pellaux (2004) Piezoelectric $Pb(Zr_x, Ti_{1-x})O_3$ thin film cantilever and bridge acoustic sensors for miniaturized photoacoustic gas detectors. Journal of Micromechanics and Microengineering14(12):1650–1658.

Lee, B. W., E. J. Lee (2006) Effects of complex doping on microstructural and electrical properties of PZT ceramics. Journal of Electroceramics 17(2-4):597–602.

Malik, R. A., A. Hussain, A. Maqbool, A. Zaman, T. K. Song, W. J. Kim & M. H.Kim (2016) Giant strain, thermally-stable high energy storage properties and structural evolution of Bi-based lead-free piezoceramics.Journal of Alloys and Compounds 682: 302-310.

Nguyen, M. D., T. Q. Trinh, M. Dekkers, E. P. Houwman, H. N. Vu & G. Rijnders (2014) Effect of dopants on ferroelectric and piezoelectric properties of lead zirconatetitanate thin films on Si substrates. Ceramics International 40(1, pt. A):1013–1018.

Nonaka, K., M. Akiyama, C-N.Xu, T. Hagio, M. Komatsu & A. Takase (2000) Enhanced Photovoltaic Response in Lead Lanthanum Zirconate-Titanate Ceramics with A-Site Deficient Composition for Photostrictor Application. Japanese Journal of Applied Physics 39(9):5144–5145.

Ohtaka, O., R. Mühll, J.Ravez (1995) Low-temperature sintering of $Pb(Zr,Ti)O_3$ ceramics with the Aid of oxyfluoride Additive: X-Ray diffraction and dielectric studies. Journal of the American Ceramic Society 78 (3): 805-808.

Pereira, M., A. G. Peixoto, M. J. M. Gomes (2001) Effect of Nb doping on the microstructural and electrical properties of the PZT ceramics.Journal of the European Ceramic Society 21(10-11): 1353–1356.

Praveen, J. P., T. Karthik, A.R. James, E. Chandrakala, S. Asthana& D. Das (2015)Effect of poling process on piezoelectric properties of sol–gel derived BZT–BCT ceramics. Journal of the European Ceramic Society 35(6):1785-1798.

Raí, R., S. Sharma, R. N. P. Choudhary (2005) Dielectric and piezoelectric studies of Fe doped PLZT ceramics. Materials Letters 59 (29-30): 3921-3925.

Saha, S. K., D. C. Agrawal (1992) Composition fluctuations and their influence on the properties of lead zirconatetitanate ceramics. American Ceramic Society Bulletin 71(9): 1424-1428.

Sakaki, C., B. L. Newalkar, S. Komarneni, K. Uchino (2001) Grain size dependence of high power piezoelectric characteristics in Nb doped lead zirconatetitanate oxide ceramics. Japanese Journal of Applied Physics 40(12):6907–6910.

Shrout, T. R., S. J. Zhang (2007) Lead-free piezoelectric ceramics: Alternatives for PZT Journal of Electroceramics 19(1):113–126.

Singh, V., H. H. Kumar, D. K. Kharat, S. Hait, M.P. Kulkarni (2006) Effect of Lanthanum substitution on ferroelectric properties of Niobium doped PZT ceramics. Materials Letters 60(24):2964–2968.

Sriram, S., M .Bhaskaran, A. Mitchell (2010) Piezoelectric thin film deposition: novel self-assembled island structures and low temperature processes on silicon 1, in Piezoelectric Ceramics. Ed. E.S. Gómez, Rijeka (Croatia), Sciyo, pp.1-21.

Tadon, R. P., V. Singh (1994) Properties of low temperature sintered neodymium doped lead zirconatetitanate ceramics. Journal of Materials Science Letters 13(11):810-812.

Takahashi S. (1982) Effects of impurity doping in lead zirconate-titanate ceramics. Ferroelectrics 41(1): 143-156.

Weston, T. B., A. H. Webster, V. M. McNamara (1969) Lead zirconatetitanate piezoelectric ceramics with iron oxide additions. Journal of The American Ceramic Society 52(5): 253–257.

Wilkinson, A. P., J. Xu, Pattanaik S, S. J. L. Billinge (1998) Neutron Scattering Studies of Compositional Heterogeneity in Sol-Gel Processed Lead ZirconateTitanates. Chemistry of Materials 10(11) :3611–3619.

Wongmaneerung, R, R. Tipakontitikul, P. Jantaratana, A. Bootchanont, J. Jutimoosik, R. Yimnirun& S. Ananta (2016) Structure and phase formation behavior and dielectric and magnetic properties of lead iron tantalite-leadzirconatetitanatemultiferroic ceramics. Materials Research Bulletin 75:91-99.

Yu, L., H. Deng, W. Zhou (2017) Influence of B site-cations on phase transition, magnetic switching and band-gap modulation in $Pb(B'_{0.5}B''_{0.5})O_3$–$Pb(Zr_{0.53}Ti_{0.47})O_3$ ceramics. Ceramics International 43(2): 2372-237.